

Sc(III) porphyrins. The molecular structure of two Sc(III) porphyrins and a re-evaluation of the parameters for the molecular mechanics modelling of Sc(III) porphyrins

Alvaro S. de Sousa^{a,*}, Manuel A. Fernandes^a, Winston Nxumalo^a, James L. Balderson^a, Tanya Jeftić^a, Ignacy Cukrowski^b, Helder M. Marques^{a,*}

^a Molecular Sciences Institute, School of Chemistry, University of the Witwatersrand, PO Wits, Johannesburg 2050, South Africa

^b Department of Chemistry, University of Pretoria, Pretoria 0002, South Africa

Received 18 January 2007; received in revised form 8 February 2007; accepted 10 February 2007

Available online 21 February 2007

Abstract

The crystal structures of two new Sc(III) porphyrins, [Sc(TPP)Cl]·2.5(1-chloronaphthalene), (5,10,15,20-tetraphenylporphyrin)-chloro-scandium(III)-2.5(1-chloronaphthalene) solvate, (Mo K α , 0.71073 Å, triclinic system $P\bar{1}$, $a = 9.9530(2)$ Å, $b = 15.4040(3)$ Å, $c = 17.7770(3)$ Å, $\alpha = 86.5190(10)^\circ$, $\beta = 89.7680(10)^\circ$, $\gamma = 86.9720(10)^\circ$, 13101 independent reflections, $R_1 = 0.0712$) and the dimeric [μ_2 -(OH) $_2$ (Sc(TPP)) $_2$], bis-(μ -hydroxo)-(5,10,15,20-tetraphenylporphyrin) scandium(III) (Mo K α , 0.71073 Å, monoclinic system $C2$, $a = 24.2555(16)$ Å, $b = 11.1598(7)$ Å, $c = 25.6468(17)$ Å, $\beta = 91.980(2)^\circ$, 13084 independent reflections, $R_1 = 0.0485$) are reported. In [Sc(TPP)Cl] the metal is five-coordinate and the porphyrin is domed with the metal displaced by 0.63 Å from the mean porphyrin towards the axial Cl⁻ ligand. The average Sc–N bond length is 2.143(3) Å, which is shorter than the average bond length of previously reported structures. Two of the phenyl rings are nearly orthogonal to the porphyrin core and the other two are significantly tilted because of contacts with 1-chloronaphthalene solvent molecules, and the phenyl rings of neighbouring porphyrins. In [μ_2 -(OH) $_2$ (Sc(TPP)) $_2$] both porphyrins are domed, with the metal displaced from the mean porphyrin plane towards the bridging hydroxo ligands. The average Sc–N bond length is 2.197(12) Å, which is in the upper range of Sc–N bond lengths in known Sc(III) porphyrins but not dissimilar to the average Sc–N bond lengths in another other bis- μ_2 -hydroxo Sc(III) porphyrin, [μ_2 -(OH) $_2$ (Sc(OEP)) $_2$]. One porphyrin is rotated relative to the upper porphyrin by 25° due to steric contacts between the phenyl substituents. We have used these new structures to re-evaluated our previously reported molecular mechanics force field parameters for modelling Sc(III) porphyrins using the MM2 force field; the training set was augmented from two to seven structures by using all available Sc(III) porphyrin structures and the two new structures. The modelling reproduces the porphyrin core very accurately; bond lengths are reproduced to within 0.01 Å, bond angles to within 0.5° and torsional angles to within 2°. The optimum parameters for modelling the Sc(III)–N bond lengths, determined by finding the minimum difference between the crystallographic and modelling mean bond lengths with the aid of artificial neural network architectures, were found to be 0.90 ± 0.03 mdyne Å⁻¹ for the bond force constant and 2.005 ± 0.005 Å for the strain-free bond length. Modelling the seven Sc(III) porphyrins with the new parameters gives an average Sc–N bond length of 2.182 ± 0.018 Å, indistinguishable from the crystallographic mean of 2.181 ± 0.024 Å.

© 2007 Elsevier B.V. All rights reserved.

Keywords: Metalloporphyrins; Scandium; Artificial neural networks; Force field; Molecular mechanics

Abbreviations: TPP, 5,10,15,20-tetraphenylporphyrin; TTP, 5,10,15,20-tetra-*p*-tolylporphyrin; OEP, 2,3,7,8,12,13,17,18-octaethylporphyrin.

* Corresponding authors. Fax: +27 11 717 6749.

E-mail addresses: Alvaro.Desousa@wits.ac.za (A.S. de Sousa), Helder.Marques@wits.ac.za (H.M. Marques).

1. Introduction

We have previously [1] reported parameters for the modelling of the porphyrin core of iron porphyrins using molecular mechanics methods and the MM2 force field

[2]. The development of the parameters was based on the results of a survey of all crystal structures of iron porphyrins available in the Cambridge Structural Database (CSD) at the time and the experience we had acquired in the modelling of the cobalt corrinoids [3]. The force field we developed reproduced porphyrin core bond lengths to better than 0.01 Å, bond angles to better than 2.5° and torsional angles to better than 4.5° of the mean crystallographic values; these results are within one standard deviation of the mean of the experimental results. With very minor modifications, we have found that these parameters in fact adequately reproduce the structural parameters of all metalloporphyrins of the first transition series [4–7].

In an endeavour to obtain a set of reliable parameters that can be used to explore metalloporphyrins structures of all metalloporphyrins of the *d* block, we have focussed on the development of metal–porphyrin ($M-N_{\text{porph}}$) bond stretching parameters and have used artificial neural networks to assist in the rapid development of these parameters. We have reported parameters for modelling four coordinate Cu(II), Co(II), Ni(II), Pd(II) [4] and Zn(II) [5] porphyrins; five-coordinate Zn(II) porphyrins [6]; and the metalloporphyrins of Sc, Ti, V and Cr in all oxidation states and with all coordination geometries of the metal [6], and of five- and six-coordinate porphyrins of all oxidation states of Mn, Co, Ni and Cu [7].

In some cases, very few structures were available so that the parameters we have reported were necessarily preliminary parameters. One such case was for Sc(III) porphyrins where the training set consisted of only two structures, [Sc(OEP)(Me)] [8] and [Sc(OEP)(CH(SiMe₃)₂)] [8] as we had deliberately excluded dimeric porphyrins (to preclude porphyrin–porphyrin dimer interactions skewing the structural data) and porphyrins in which an axial ligand is coordinated in an η^5 fashion (we have never modelled such complexes). We have now extended the training set used previously for the modelling of Sc(III) porphyrins. An examination of the structure of dimeric [μ_2 -(OH)₂(Sc(OEP))₂] (bis[μ_2 -hydroxo)-(octaethylporphyrin)-scandium] [8] showed that the porphyrins are in fact sufficiently far apart (5.05 Å) so as to have no undue effect on each other's structure. This structure has therefore now been included in the training set. Two organometallic η^5 -coordinated structures, (η^5 -cyclopentadienyl)-octaethylporphyrin-scandium, [Sc(OEP)(cp)] [9], and (η^5 -indenyl)-(octaethylporphyrin)-scandium, [Sc(OEP)(ind)] [8], have been reported. We have shown previously that parameters for the equatorial $M-N_{\text{porph}}$ bond are rather insensitive to the value of the parameters for the axial $M-N_{\text{axial}}$ bond. We have therefore developed preliminary parameters for modelling these organometallic complexes and also incorporated the two structures in the training set.

Two other Sc(III) porphyrin structures, [Sc(TTP)Cl] and [μ_2 -(O)(Sc(TTP))₂] have been reported [10] but only incomplete coordinates are available in the CSD. We could not include these in the training set.

We report here the structure of two new Sc(III) porphyrins, [Sc(TPP)Cl] and [μ_2 -(OH)₂(Sc(TPP))₂]. These have been included in the training set which has therefore been augmented from 2 to 7 structures. We have re-determined the optimum Sc(III)– N_{porph} bond stretching parameter, and report on this in this paper.

2. Methods

2.1. Crystallography

Intensity data were collected on a Bruker APEX II CCD area detector diffractometer with graphite monochromated Mo *K* α radiation (50 kV, 30 mA) using the APEX 2 [11] data collection software. The collection method involved ω -scans of width 0.5° and 512 × 512 bit data frames. Data reduction was carried out using *SAIN*T+ [12]. Diagrams and publication material were generated using *SHELX*TL, *PLATON* [13], and *ORTEP*-3 [14].

2.1.1. [Sc(TPP)Cl]

The crystal structure was solved by direct methods using *SHELX*TL [15]. Non-hydrogen atoms were first refined isotropically followed by anisotropic refinement by full matrix least-squares calculations based on F^2 using *SHELX*TL. Where possible hydrogen atoms were first located in the difference map then positioned geometrically and allowed to ride on their respective parent atoms. One of the phenyl groups on the main molecule was found to be disordered and in the final refinements was refined over two positions with the final occupancies being 0.36(3) and 0.64(3) for each orientation, respectively. The structure contains three disordered chloronaphthalene molecules in three different sites in the structure. The first of these was refined over two positions using *SADI*, *FLAT*, *SIMU* and *DELU* restraints. The second molecule was found to be disordered in at least three orientations and was refined in three orientations as rigid bodies. The third molecule was similarly disordered over at least two orientations over a centre of inversion making the use of disorder models extremely difficult. Consequently, the structure was processed with *SQUEEZE* [16], which accounted for 80 electrons, close to the 84 required for a chloronaphthalene molecule. In the final refinements, the contribution of the chloronaphthalene molecule to the structure was added to $F(000)$, crystal density and unit cell contents values.

2.1.2. [μ_2 -(OH)₂(Sc(OEP))₂]

The crystal structure was solved by direct methods using *SHELX*TL [15]. Non-hydrogen atoms were first refined isotropically followed by anisotropic refinement by full matrix least-squares calculations based on F^2 using *SHELX*TL. Hydrogen atoms were first located in the difference map then positioned geometrically and allowed to ride on their respective parent atoms. All but one of the eight phenyl groups in the structure were disordered. Each of these was refined as rigid bodies over two positions with the

sum of the final occupancies being constrained to one. In addition, it was found that the hydroxo groups attached to the scandium atoms were also disordered. These were refined over three positions using SADI and FLAT restraints with the sum of the final occupancies also being constrained to one. The final occupancies were 0.526(16), 0.129(6) and 0.306(15) for the pairs of atoms O1 and O2, O1A and O2A, and O1B and O2B, respectively.

2.2. Molecular modelling

Molecular mechanics (MM) modelling was performed with the version of MM2 [2] called MM+ in the HYPER-CHEM suite of programmes [17]. The potential energy functions used have been listed previously [1] and the atom type definitions are given in Table S1 of the Supplementary Information. The porphyrin core was modelled with the parameters that we have previously reported [4,5]. Standard MM2 parameters were used as required for modelling organic substituents on the porphyrin ring and the axial ligands, and no MM+ parameters were used in the modelling.

Modelling of the bonding to coordinated cyclopentadienyl in [Sc(OEP)(cp)] and to indenyl in [Sc(OEP)(ind)] was performed as follows. The Sc–C distance observed crystallographically is 2.51 ± 0.03 Å. We set the strain-free Sc–C bond length to the crystallographic mean and used a bond stretch constant of 0.50 mdyn Å⁻¹. Since MM+ uses a “points-on-a-sphere” model, all bond angles of the type X–M–Y, where M is greater than 4-coordinate are ignored. All torsions involving the Sc–C bond were set to zero. This approach adequately reproduced the Sc–C bond distances (2.51 ± 0.05 Å) with the mean plane through the alkyl ligand and that through the porphyrin core remaining parallel as observed in the solid state structures.

Because of the use of the “points-on-a-sphere” model implemented in MM+, and which, as previously described [3,6,7], we have found to be inadequate for modelling the structures of both cobalamins [3] and metalloporphyrins [6,7], we added parabolic restraints to the force field to model bond angles of the type X–Sc–Y; these are listed in Table S2 of the Supplementary Information. The values of the bond angles and torsions used were the crystallographic mean of the seven structures used in the training set; the force constants were those used previously [6,7].

All dipole moments involving the metal ion were set to zero. Unless otherwise indicated, the crystal structure was used as the starting point for the calculations. The strain energy was minimised using firstly 1000 cycles of a steepest descent algorithm followed by a Polak–Ribiere conjugate gradient algorithm with a convergence criterion of $r.m.s.d. < 0.01$ kcal mol⁻¹ Å⁻¹ in the gradient. Minimisation usually occurred within 800 cycles of the latter algorithm.

The extent of the distortion of each porphyrin from planarity, D_{oop} , was quantified in terms of the normal-coordi-

nate structural decomposition (NSD) procedure developed by Jentzen, Song and Shelnutz [18].

2.3. Artificial neural network architectures

To derive the M–N_{porph} bond parameters, the values of the strain-free bond length, l_o , and the bond stretching force constant, k_s , were varied in a grid-like pattern for values of (i) l_o between 1.85 and 2.10 Å and (ii) values of k_s between 0.1 and 1.5 mdyn Å⁻¹. We defined the error function as the mean difference between the modelled and the crystallographically observed M–N_{porph} bond lengths, and determined its dependence on l_o and k_s . This range of l_o and k_s provided a preliminary grid upon which to base the artificial neural networks (ANN) calculations. These initial points were supplemented with additional points as the shape of the error function emerged. These calculations were performed using WinNN32 [19], as previously described [4–7]. ANN architectures that gave similar results were used to generate the error response surfaces and compute the optimum values of l_o and k_s . The predicted global minimum was computed by averaging the l_o and k_s values from those trained ANN architectures where the predicted error in the M–N_{porph} bond length was the smallest. The standard deviations for the l_o and k_s values and the expected error in the average computed M–N bond length were calculated from the ANN results.

2.4. Synthesis

The synthesis of (5,10,15,20-tetraphenylporphyrin)-chloro-scandium(III), [Sc(TPP)Cl], was a modification of the methods described by Arnold et al. [8] and by Sewchok et al. [10]. A mass of 1.1 g H₂TPP (Strem, 1.9 mmol) was added to 13 mL 1-chloronaphthalene (Aldrich). The solution was degassed using three freeze-thaw cycles,

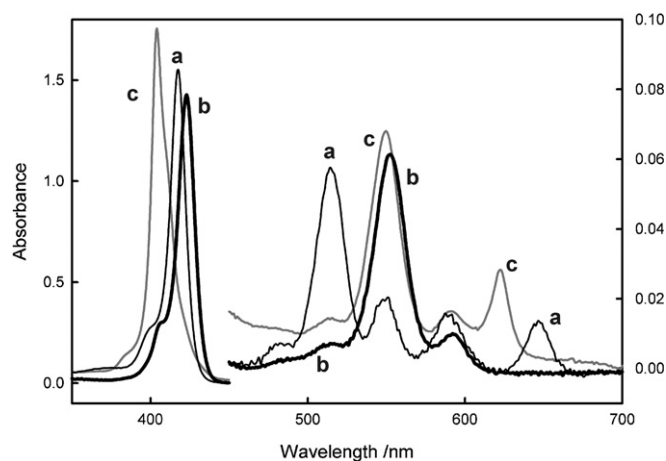


Fig. 1. UV-visible spectrum of (a) [H₂TPP], (b) [Sc(TPP)Cl] and (c) [μ₂-(OH)₂(Sc(TPP))₂] in dichloromethane.

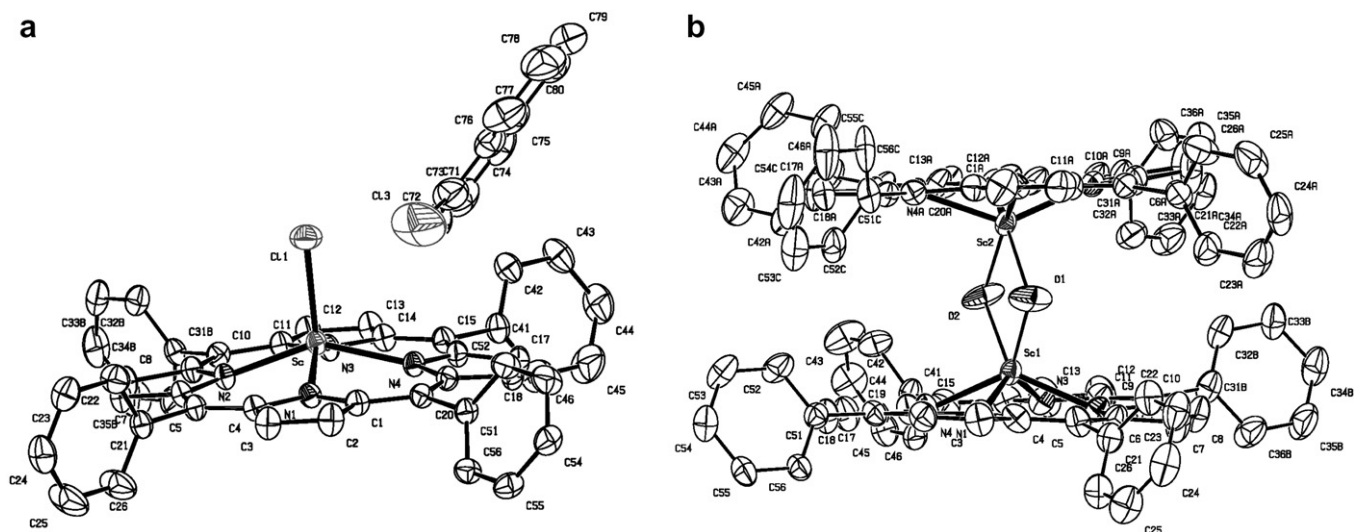


Fig. 2. (a) ORTEP diagram of $[\text{Sc}(\text{TPP})\text{Cl}]\cdot 2.5(1\text{-chloronaphthalene})$, with the major conformation of the porphyrin and one of the orientations of 1-chloronaphthalene in one of the solvent sites (see Fig. S1 of the Supplementary Information) for a diagram showing all conformations of the porphyrin and the disordered solvent molecules in two sites. (b) ORTEP diagram showing one conformation of the dimeric porphyrin $[\mu_2\text{-(OH)}_2(\text{Sc}(\text{TPP}))_2]$. See Fig. S1 of the Supplementary Information. Hydrogen atoms have been omitted for clarity.

purged with Ar, refluxed for 2 h under a CaCl_2 drying tube, and then further degassed twice with an Ar purge. ScCl_3 (Aldrich), 1.1 g (7.3 mmol), was added to the solution.

The flask was evacuated and purged with Ar, and then heated and refluxed for 2 h. During the reflux, the reaction flask was regularly evacuated and purged with Ar to

Table 1
Experimental data for the crystal structure determination of $[\text{Sc}(\text{TPP})\text{Cl}]$ and $[\mu_2\text{-(OH)}_2(\text{Sc}(\text{TPP}))_2]$ reported in this work

	$[\text{Sc}(\text{TPP})\text{Cl}]$	$[\mu_2\text{-(OH)}_2(\text{Sc}(\text{TPP}))_2]$
CSD deposit number	633411	633412
Moiety formula	$\text{C}_{44}\text{H}_{28}\text{ClN}_4\text{Sc}, 2.5(\text{C}_{10}\text{H}_7\text{Cl})$	$\text{C}_{88}\text{H}_{58}\text{N}_8\text{O}_2\text{Sc}_2$
Formula weight	1099.63	1349.34
Temperature (K)	173(2) K	123(2) K
Wavelength (Å)	0.71073 Å	0.71073 Å
Crystal system	Triclinic	Monoclinic
Space group	$P\bar{1}$	$C2$
Unit cell dimensions/Å	$a = 9.9530(2)$ $b = 15.4040(3)$ $c = 17.7770(3)$ $\alpha = 86.5190(10)^\circ$ $\beta = 89.7680(10)^\circ$ $\gamma = 86.9720(10)^\circ$	$a = 24.2555(16)$ $b = 11.1598(7)$ $c = 25.6468(17)$ $\beta = 91.980(2)^\circ$
Volume (Å ³)	2716.67(9)	6938.1(8)
Z	2	4
D_{calc} (mg m ⁻³)	1.344	1.292
μ (mm ⁻¹)	0.356	0.253
$F(000)$	1136	2800
Crystal dimensions (mm ³)	$0.48 \times 0.20 \times 0.11$	$0.50 \times 0.21 \times 0.03$
θ range for data collection/ $^\circ$	1.15 to 28.00	0.79 to 26.00
Index ranges	$-13 \leq h \leq 13$ $-20 \leq k \leq 20$ $-23 \leq l \leq 23$	$-25 \leq h \leq 29$ $-13 \leq k \leq 13$ $-31 \leq l \leq 31$
Reflections collected	51095	33248
Independent reflections	13101 [$R(\text{int}) = 0.0276$]	13084 [$I(\text{int}) = 0.0596$]
Refinement method	Full-matrix least-squares on F^2	Full-matrix least-squares on F^2
Data/restraints/parameters	13101/1051/670	13084/1403/1148
Goodness-of-fit on F^2	1.110	0.993
Final R indices [$I > 2\sigma(I)$]	$R_1 = 0.0712$, $wR_2 = 0.2058$	$R_1 = 0.0485$, $wR_2 = 0.0930$
R indices (all data)	$R_1 = 0.0859$, $wR_2 = 0.2190$	$R_1 = 0.1095$, $wR_2 = 0.1162$
Largest diff. peak and hole/e Å ³	1.233/−0.864	0.284 and −0.398

remove the HCl formed. The solution turned violet on completion of the reaction.

The product crystallises as purple crystals if the solution is allowed to cool. Just before that occurred, the solution was filtered under reduced pressure to remove unreacted ScCl₃ whilst preventing co-precipitation of the complex. The solution was then allowed to cool down to room temperature and was refrigerated (at 5 °C) for 12 h. The product was filtered, washed with 1 mL of 1-chloronaphthalene and 4 × 10 mL aliquots of hexane, and air-dried to obtain a purple solid (1.148 g, 92% yield). To obtain diffraction-quality crystals, the product was dissolved in a minimum volume of degassed (Ar) 1-chloronaphthalene and slowly cooled.

We synthesised [Sc(TPP)Et] using the procedure described by Arnold et al. [8] for the synthesis of [Sc(OEP)Me]. All glassware was heated under reduced pressure to approximately 300 °C with the aid of a heat gun; on cooling to ambient temperature it was purged with argon that had been passed through dry silica gel. This procedure was repeated twice before 5 mL of dry diethylether was added by injection through a septum and degassed. To this continuously stirred solution was added a solution of ethylmagnesium chloride (0.8 mL of 2.0 M, 1.6 mmol) in diethylether. Anhydrous dioxane (0.16 mL, 1.94 mmol) was then added dropwise by means of a gas-tight syringe to the reaction mixture. The solution was stirred for a further 8 h to ensure complete formation of diethylmagnesium. The ether solvent, in which Et₂Mg was dissolved, was removed under reduced pressure and the reaction flask purged with argon.

Anhydrous toluene (8 mL) was placed in a separately dried Schlenk tube and degassed by twice by repeating freeze-thaw cycles, of approximately 25 min each, under reduced pressure and purging with argon each time. To the dry, degassed toluene a non-stoichiometric amount of [Sc(TPP)Cl] was added (250 mg, 0.104 mmol) followed by a single degassing freeze-thaw cycle. The resulting violet solution was cannula transferred to the reaction flask containing the diethylmagnesium and was continuously stirred for 14 h. Filtration of the reaction solution through a sintered glass frit under inert conditions and removal of all solvents under reduced pressure resulted in an air-stable crimson powder of [Sc(TPP)Et] (232.8 mg, 94%).

Several attempts were made at recrystallising [Sc(TPP)Et] from a variety of solvents. We only obtained red crystals of bis-μ-hydroxo dimeric porphyrin, [μ₂-(OH)₂(Sc(TPP))₂], despite all efforts to exclude moisture. Attempts to crystallise [Sc(TPP)Et] are continuing and, if successful, the structure will be reported elsewhere.

3. Results and discussion

3.1. [Sc(TPP)Cl]

The UV–visible spectrum of [Sc(TPP)Cl] in dichloromethane (Fig. 1) shows a shift in the Soret band from

418 nm for [H₂TPP] to 422 nm. In the visible region, the four bands at 515, 552, 592 and 640 nm in the spectrum of [H₂TPP] are replaced by bands at 517, 554 and 593 nm, with the central band being the most intense. The FT-IR spectrum of [Sc(TPP)Cl] shows a strong band at 422 cm⁻¹, which is characteristic of a Sc–N stretch, reported at 417 cm⁻¹ for [Sc(TTP)Cl] [10]. FAB-MS(M⁺) gave the most intense peak at *m/z* 657.2, which corresponds to loss of the chloride from the complex.

3.2. [Sc(TPP)Et]

The UV–visible spectrum in hexane shows the Soret band at 404 nm with four bands in the visible region appearing at 513, 549, 589 and 622 nm (Fig. 1). As for [Sc(TPP)Cl], the FAB-MS(M⁺) spectrum showed the most

Table 2
Bond lengths (Å) and bond angles (°) of the coordination sphere of Sc(III) of the Sc(III) porphyrins reported in this work

[Sc(TPP)Cl]		[μ ₂ -(OH) ₂ (Sc(TPP)) ₂]	
Sc–N(1)	2.145(3)	N(1)–Sc(1)	2.186(3)
Sc–N(2)	2.139(3)	N(2)–Sc(1)	2.210(3)
Sc–N(3)	2.144(3)	N(3)–Sc(1)	2.190(3)
Sc–N(4)	2.145(3)	N(4)–Sc(1)	2.199(3)
		N(1A)–Sc(2)	2.204(3)
		N(2A)–Sc(2)	2.180(3)
		N(3A)–Sc(2)	2.213(3)
		N(4A)–Sc(2)	2.192(2)
Cl(1)–Sc	2.3482(12)	O(1)–Sc(1)	2.053(8)
		O(1)–Sc(2)	2.077(7)
		O(2)–Sc(2)	2.044(8)
		O(2)–Sc(1)	2.077(7)
N(2)–Sc–N(3)	84.79(11)	N(1)–Sc(1)–N(2)	82.47(10)
N(2)–Sc–N(1)	85.48(11)	N(1)–Sc(1)–N(4)	80.64(11)
N(3)–Sc–N(4)	85.31(11)	N(3)–Sc(1)–N(2)	81.29(11)
N(1)–Sc–N(4)	84.79(11)	N(3)–Sc(1)–N(4)	82.98(12)
		N(2A)–Sc(2)–N(1A)	82.48(12)
		N(4A)–Sc(2)–N(1A)	81.43(11)
		N(2A)–Sc(2)–N(3A)	80.99(11)
		N(4A)–Sc(2)–N(3A)	82.44(10)
N(3)–Sc–N(1)	145.37(12)	N(1)–Sc(1)–N(3)	137.24(12)
N(2)–Sc–N(4)	146.60(12)	N(4)–Sc(1)–N(2)	134.20(12)
		N(1A)–Sc(2)–N(3A)	133.96(12)
		N(2A)–Sc(2)–N(4A)	137.42(11)
N(2)–Sc–Cl(1)	106.61(9)	O(1)–Sc(1)–O(2)	69.4(3)
N(3)–Sc–Cl(1)	107.63(9)	O(2)–Sc(2)–O(1)	69.6(3)
N(1)–Sc–Cl(1)	107.00(9)	O(1)–Sc(1)–N(1)	87.1(4)
N(4)–Sc–Cl(1)	106.79(9)	O(2)–Sc(1)–N(1)	131.6(4)
		O(1)–Sc(1)–N(2)	88.6(3)
		O(2)–Sc(1)–N(2)	135.6(4)
		O(1)–Sc(1)–N(3)	131.5(4)
		O(2)–Sc(1)–N(3)	85.5(3)
		O(1)–Sc(1)–N(4)	132.4(4)
		O(2)–Sc(1)–N(4)	85.1(3)
		O(1)–Sc(2)–N(1A)	80.2(3)
		O(2)–Sc(2)–N(1A)	144.9(3)
		O(1)–Sc(2)–N(2A)	99.1(4)
		O(2)–Sc(2)–N(2A)	118.9(4)
		O(1)–Sc(2)–N(3A)	144.8(3)
		O(2)–Sc(2)–N(3A)	79.5(3)
		O(1)–Sc(2)–N(4A)	116.5(5)
		O(2)–Sc(2)–N(4A)	96.0(4)

intense peak at m/z 657.2, indicating loss of the axial ligand. In solution, the complex is air and moisture-sensitive; exposure to the atmosphere results in formation of a new species, which we have subsequently found to be a bis- μ -hydroxo dimer (see below) as evidenced by the formation of a shoulder on the Soret band at 419 nm when the spectrum is recorded in dry hexane or dry diethylether which is left exposed to the atmosphere (Fig. S1 of the Supplementary Information). In the visible region, the band at 622 nm disappears, whilst the other three bands do not change position, but their intensity drops. The conversion of [Sc(TPP)Et] to the bis- μ -hydroxo dimer is typically complete within 3 h under these conditions.

3.3. Structure of [Sc(TPP)Cl]

[Sc(TPP)Cl] crystallises in the $P\bar{1}$ space group ($R_1 = 7.12\%$, Fig. 2). The experimental data are summarised in Table 1. Some of the bond lengths and angles involving the metal ion are summarised in Table 2.

Two of the phenyl rings of the porphyrin in [Sc(TPP)Cl] are nearly orthogonal to the porphyrin core (the torsion angles about the meso C–phenyl bond are 82° and 80° , respectively) whilst the other two are significantly tilted (torsion angles are 61° and 71° , respectively) because of contacts between H atoms on the phenyl substituents and those on the 1-chloronaphthalene solvent molecules, and between the phenyl rings of two neighbouring porphyrins.

Like all other monomeric Sc(III) porphyrins reported to date, the metal is five-coordinate and the porphyrin is

domed with the metal displaced by 0.63 \AA from the mean porphyrin towards the axial ligand. An analysis of the porphyrin deformation using the NSD procedure [18] shows a total deformation of $D_{\text{oop}} = 1.25 \text{ \AA}$ from planarity, consisting mostly of doming, although there is also some wave deformation.

The average Sc–N bond length is $2.143(3) \text{ \AA}$, which is shorter than the average bond length of previously reported structures ($2.183 \pm 0.021 \text{ \AA}$); indeed, only one other structure, [Sc(OEP)(CH(SiMe₃)₂)] [8], has Sc–N bonds that are of comparable length (two Sc–N bond lengths are 2.142 \AA and the other two are 2.150 \AA).

3.4. Structure of $[\mu_2\text{-(OH)}_2\text{(Sc(TPP))}_2]$

The dimeric porphyrin crystallises in the $C2$ space group (Table 1). Both porphyrins are significantly distorted from planarity ($D_{\text{oop}} = 1.27$ and 1.65 \AA , respectively). As with [Sc(TPP)Cl], the major deformation is doming; there is some wave deformation and also saddling of the two porphyrins.

The average Sc–N bond length (Table 2) is $2.197 \pm 0.012 \text{ \AA}$, which is in the upper range of Sc–N bond lengths in Sc(III) porphyrins reported prior to this work ($2.181 \pm 0.024 \text{ \AA}$) but not dissimilar to the average Sc–N bond lengths in the other bis- μ_2 -hydroxo Sc(III) porphyrin reported previously, $[\mu_2\text{-(OH)}_2\text{(Sc(OEP))}_2]$, $2.203 \pm 0.008 \text{ \AA}$ [8]. The structures of the two dimeric porphyrins are similar (Fig. 3) except that, in the case of $[\mu_2\text{-(OH)}_2\text{(Sc(TPP))}_2]$, the lower porphyrin is rotated relative to the upper porphyrin by 25° in a clockwise direction

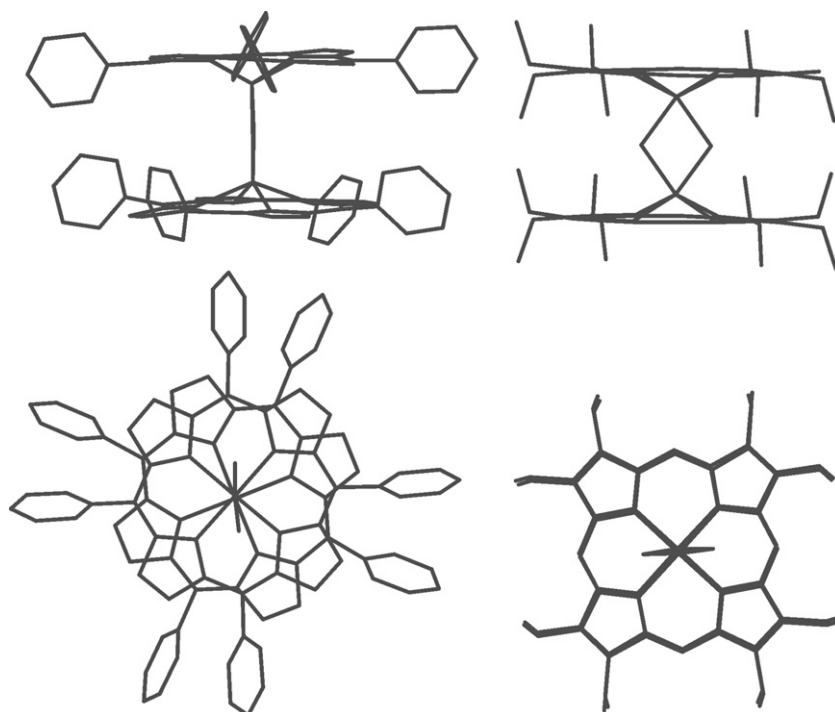


Fig. 3. Two views of the structures of (left) $[\mu_2\text{-(OH)}_2\text{(Sc(TPP))}_2]$ and (right) of $[\mu_2\text{-(OH)}_2\text{(Sc(OEP))}_2]$. Hydrogen atoms are omitted for clarity.

whereas in $[\mu_2\text{-(OH)}_2\text{(Sc(OEP))}_2]$ the projection of the two porphyrins are virtually coincidental (their relative rotation is less than 2°). This is almost certainly due to steric contacts between the phenyl substituents in the former, even though they are significantly tilted from the vertical (the mean torsion about the meso C–phenyl bond is $67 \pm 5^\circ$). The tilting of the phenyl groups is also likely to be due to contacts between hydrogen atoms of the phenyl groups on neighbouring molecules in the structure, i.e., packing effects.

3.5. Molecular modelling

The average Sc–N bond length in the seven porphyrin structures on which the molecular modelling was based (5 monomeric porphyrins, 2 dimeric porphyrins, 36 Sc–N bond lengths reported) is $2.181 \pm 0.024 \text{ \AA}$. To determine

the optimum values for the Sc–N bond parameters, k_s and l_o , they were varied between 1.75 and 2.15 \AA , and 0.1 and $1.5 \text{ mdyn \AA}^{-1}$, respectively. In a plot of l_o against k_s (Fig. 4a), the error function has a valley of minimum values that runs diagonally from (large k_s , long l_o) to (small k_s , short l_o), showing that the two parameters are correlated.

Thus, for example, a value of $k_s = 1.35 \text{ mdyn \AA}^{-1}$ and $l_o = 2.10 \text{ \AA}$ produces a mean value of $2.172 \pm 0.007 \text{ \AA}$ for the Sc–N bond length, or a difference of 0.009 \AA between this mean value and the crystallographic mean, well within the experimental standard deviation of 0.024 \AA . A value of $k_s = 0.30 \text{ mdyn \AA}^{-1}$ and $l_o = 1.80 \text{ \AA}$ gives $2.187 \pm 0.008 \text{ \AA}$ for the Sc–N bond length, which is merely 0.006 \AA different from the crystallographic mean. This strong correlation between k_s and l_o , and the fact that there is an appreciable variation in the range of experimentally observed Sc–N bond lengths, means it is difficult to pinpoint the best val-

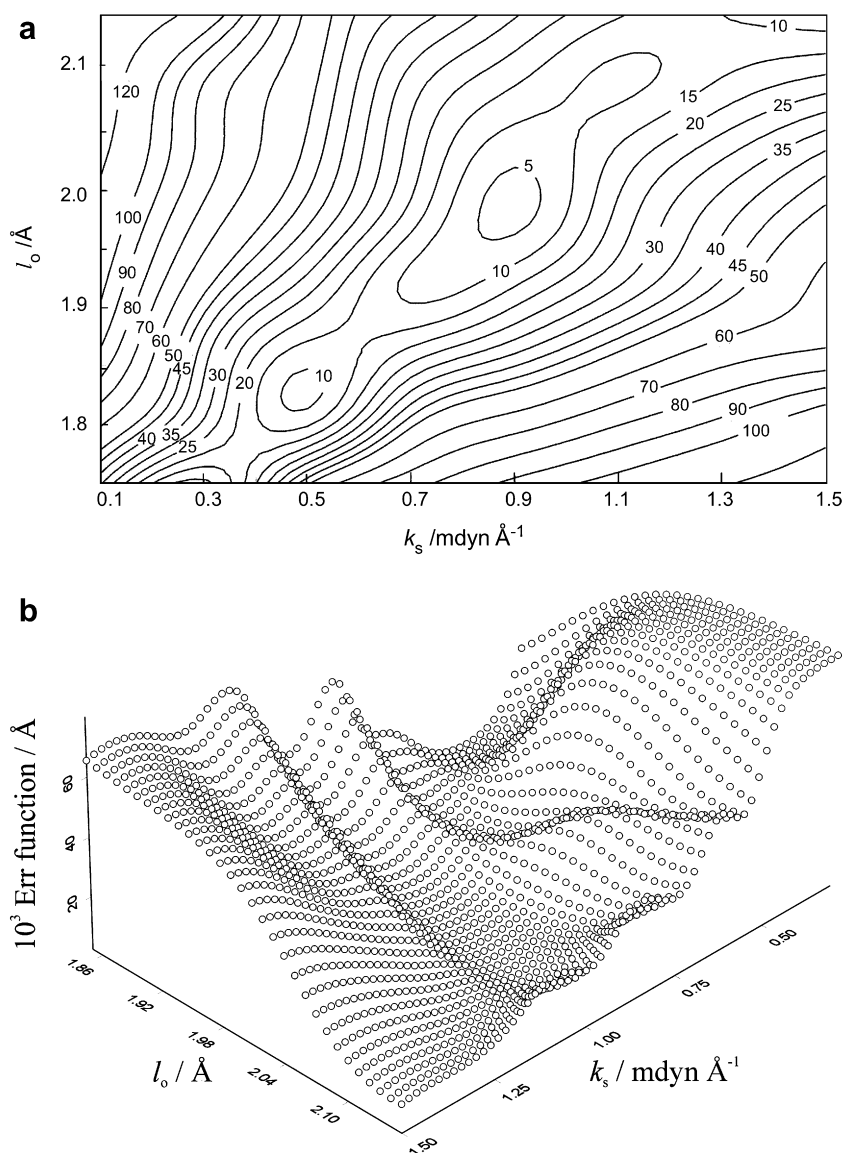


Fig. 4. ANN fit of the error function for the Sc–N bond length in the modelling of Sc(III) porphyrins. The minimum occurs at $k_s = 0.90 \text{ mdyn \AA}^{-1}$ and $l_o = 2.005 \text{ \AA}$. (a) A contour plot and (b) the three-dimensional plot.

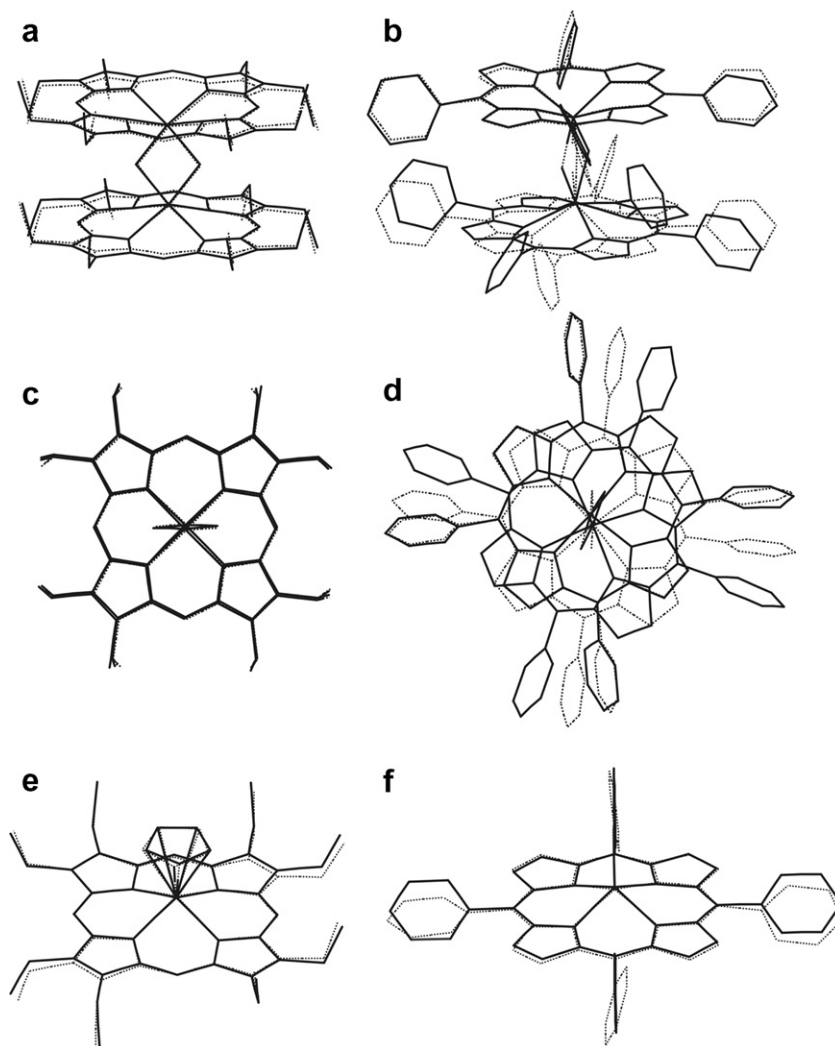


Fig. 5. Overlay of the molecular mechanics (—) and crystal structure (...) of (a and c) $[\mu_2\text{-(OH)}_2\text{(Sc(OEP))}_2]$; (b and d) $[\mu_2\text{-(OH)}_2\text{(Sc(TPP))}_2]$; (e) $[\text{Sc(OEP)(cp)}]$; and (f) $[\text{Sc(TPP)Cl}]$. Hydrogen atoms are omitted for clarity.

ues of k_s and l_o . The trained ANN architectures predicted the minimum in the error function (Fig. 4b) to occur with $k_s = 0.90 \pm 0.03 \text{ m dyn } \text{\AA}^{-1}$ and $l_o = 2.005 \pm 0.005 \text{ \AA}$. Modelling the seven Sc(III) porphyrins with these values gives an average Sc–N bond length of $2.182 \pm 0.018 \text{ \AA}$, in excellent agreement with the crystallographic mean of $2.181 \pm 0.024 \text{ \AA}$.

The crystal structures of the porphyrins are well reproduced; Fig. 5 shows four as an example. In the case of $[\mu_2\text{-(OH)}_2\text{(Sc(TPP))}_2]$, one porphyrin of the dimer is twisted more relative to the other than observed in the solid state. In the case of all TPP structures, the phenyl rings minimise into structures where they are orthogonal to the porphyrin ring whereas in the crystal structures they are invariably tilted away from the normal because of close contacts with other molecules in the lattice. As we have found before [6], if $[\mu_2\text{-(OH)}_2\text{(Sc(TPP))}_2]$ is energy minimised in a lattice where all nearest neighbours are confined to their lattice positions, then the structure observed in the solid state is indeed reproduced closely.

The porphyrin core is very well reproduced by the force field, providing further evidence of the adequacy of the parameters we have developed for modelling metalloporphyrins. Bond lengths are reproduced to 0.01 \AA or better, bond angles to within 0.5° and torsional angles to within 2° Table S3 of the Supplementary Information.

4. Conclusion

We previously determined parameters for modelling Sc(III)–N bonds in Sc(III) porphyrins, based on only two structures, to be $k_s = 0.90 \text{ m dyn } \text{\AA}^{-1}$ and $l_o = 1.95 \text{ \AA}$. We have now increased the training set to seven structures by including all available Sc(III) porphyrin structures as well as providing two novel structures. This significantly increases the confidence in the parameters for modelling Sc(III)–N bonds in Sc(III) porphyrins. We find that k_s and l_o are heavily correlated and that a wide range of values of k_s and l_o will reproduce Sc(III) porphyrin structures reasonably accurately. The optimum values found for the

two parameters in this work are 0.90 ± 0.03 mdyn \AA^{-1} and 2.005 ± 0.005 \AA , respectively. The porphyrin core is accurately reproduced with the parameters we have previously reported for modelling metalloporphyrins. Modelling the seven Sc(III) porphyrins with the new parameters gives an average Sc–N bond length of 2.182 ± 0.018 \AA , indistinguishable the crystallographic mean of 2.181 ± 0.024 \AA .

Acknowledgements

This work was made possible by grants from the National Research Foundation, Pretoria, South Africa, and the University Research Committee of the University of the Witwatersrand.

Appendix A. Supplementary data

Supplementary Information available, giving definition of atom types; parameters for the parabolic restraints added to model the coordination sphere of the metalloporphyrins; comparison of mean structural metrics of crystallographic and molecular mechanics modelled structures of seven Sc(III) porphyrins. Figures shown ORTEP diagrams of $[\text{Sc}(\text{TPP})\text{Cl}] \cdot 2.5(1\text{-chloronaphthalene})$, in which there is substantial disorder in the solvent molecules and in one of the phenyl rings of the TPP core, and of $[\mu_2\text{-(OH)}_2(\text{Sc}(\text{TPP}))_2]$, in which seven of the eight the phenyl rings are distributed over two sites and the hydroxo ligands have been refined over three positions. Another figure shows UV–visible spectra of the conversion of $[\text{Sc}(\text{TPP})\text{Et}]$ to $[\mu\text{-(OH)}_2(\text{Sc}(\text{TPP}))_2]$ on exposure of a dry hexane solution to the atmosphere. Supplementary data associated

with this article can be found, in the online version, at doi:10.1016/j.molstruc.2007.02.018.

References

- [1] H.M. Marques, O.Q. Munro, N.E. Grimmer, D.C. Levendis, F. Marsicano, T. Markoulides, *J. Chem. Soc. Faraday Trans.* 91 (1995) 1741.
- [2] N.L. Allinger, *J. Am. Chem. Soc.* 99 (1977) 8127.
- [3] H.M. Marques, K.L. Brown, *Coord. Chem. Rev.* 225 (2002) 123.
- [4] H.M. Marques, I. Cukrowski, *Phys. Chem. Chem. Phys.* 4 (2002) 5878.
- [5] H.M. Marques, I. Cukrowski, *Phys. Chem. Chem. Phys.* 5 (2003) 5499.
- [6] C.E. Skopec, J.M. Robinson, I. Cukrowski, H.M. Marques, *J. Mol. Struct.* 738 (2005) 67.
- [7] C.E. Skopec, I. Cukrowski, H.M. Marques, *J. Mol. Struct.* 783 (2006) 21.
- [8] J. Arnold, C.G. Hoffman, D.Y. Dawson, F.J. Hollander, *Organometallics* 12 (1993) 3645.
- [9] J. Arnold, C.G. Hoffman, *J. Am. Chem. Soc.* 112 (1990) 8620.
- [10] M.G. Sewchok, R.C. Haushalter, J.S. Merola, *Inorg. Chim. Acta* 144 (1988) 47.
- [11] Bruker, APEX2, V. 2.0-1, Bruker AXS Inc., Madison, Wisconsin, USA, 2005.
- [12] Bruker, SAINT+, V. 6.02 (includes XPREP and SADABS), Bruker AXS Inc., Madison, Wisconsin, USA, 1999.
- [13] A.L. Spek, *J. Appl. Cryst.* 36 (2003) 7.
- [14] L.J. Farrugia, *J. Appl. Cryst.* 30 (1997) 565.
- [15] Bruker, SHELXTL, V. 5.1 (includes XS, XL, XP, XSELL), Bruker AXS Inc., Madison, Wisconsin, USA, 1999.
- [16] P. van der Sluis, A.L. Spek, *Acta Cryst.* A46 (1990) 194.
- [17] HYPERCHEM, V. 7.03, Hypercube, Inc., Gainesville, FL, 2002.
- [18] W. Jentzen, X.-Z. Song, J.A. Shelnut, *J. Phys. Chem. B* 101 (1997) 1684.
- [19] Y. Danon, WinNN32, V. 1.6, <<http://www.geocities.com/sciware/>>, e-mail: <danony@rpi.edu/>.